

Antihydrogen beam generation using storage rings

I. Meshkov^{a,*}, A. Skrinsky^b

^aJoint Institute for Nuclear Research, 141980 Dubna, Russia

^bBudker Institute of Nuclear Physics, 630090 Novosibirsk, Russia

Received 22 April 1996

Abstract

The scheme of antihydrogen beam generation is proposed. Two storage rings should be used for effective generation of antihydrogen – an antiproton ring and a small additional one for storing and cooling of positrons. This scheme has advantages compared with those discussed earlier due to the use of a longitudinal magnetic field as the focusing system of the positron ring with the positron source immersed in this field. The electron cooling of positrons is an essential part of the project. The Low Energy Antiproton Ring (LEAR) at CERN is chosen as the *basic machine* for idea demonstration and all the numerical applications are made for it.

The rate of antihydrogen generation is limited in the case discussed here by the positron source intensity. The simplest version of this scheme permits one to achieve a rate of about 3×10^4 fast (50 MeV) atoms/s and 30 slow (0.5 MeV) ones. Simultaneously such a scheme is a generator of *orthopositronium* with a productivity of about 2×10^4 and 35 “atoms”/s, correspondingly.

The particle dynamics in the positron storage ring are considered.

1. Introduction

The idea of antihydrogen \bar{H}^0 atom generation appeared soon after the realisation of the electron cooling method [1] and has been developed since that time (see Ref. [2]). The main interest in antihydrogen production is not only a philosophical one, as the generation of the simplest type of antimatter, but it also has a concrete goal: the testing of the CPT theorem by an extremely precise comparison of the spectra of hydrogen and antihydrogen atoms. The first successful experiments on the synthesis of antihydrogen atoms, performed on the LEAR antiproton storage ring at CERN in September–November 1995 [3], will undoubtedly inspire the activity of experimentalists in this field.

This paper has the purpose to attract again the attention of the high energy physics community to the possibility of the realisation of an intense antihydrogen stream generation in the nearest future.

2. The general scheme

For antihydrogen atom intense generation an antiproton ring (LEAR, in the case to be discussed) has to be supplemented with an additional one to store and to cool the positrons (Fig. 1). The scheme of generation of \bar{H}^0

atoms presented in Ref. [1] was based on two storage rings for antiprotons and positrons, and both have a conventional strong focusing system. Soon a similar scheme was proposed [4] and the idea of electron cooling of the positrons was, probably for the first time, announced.

The scheme considered here deals also with intermediate and low energy particles, however its positron ring has a

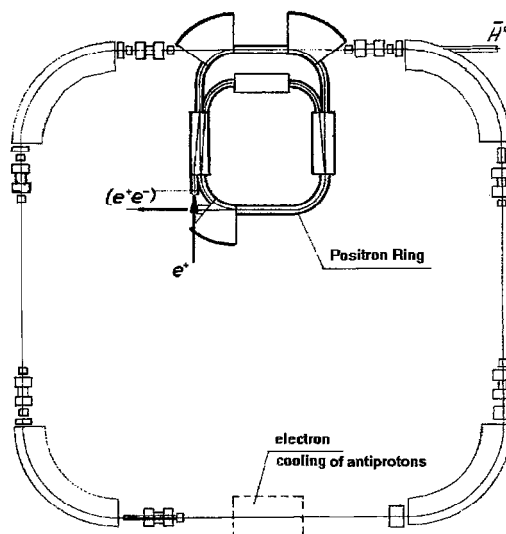


Fig. 1. Layout of LEAR-complex with the positron ring.

* Corresponding author.

focusing system with a longitudinal magnetic field. Recombination of antiproton and positron in antihydrogen occurs in this field (Section 3). Antihydrogen atoms are extracted through a vacuum channel to a spectrometric system for spectral measurements.

Both rings equipped with electron cooling devices for cooling of the antiprotons (\bar{p}) and positrons (e^+). This permits dense and cold \bar{p} and e^+ beams to be recombined. The methods of positron generation are briefly discussed below (Section 4).

A scheme with a longitudinal magnetic field and completely immersed in its positron and electron beams has some advantages. First of all, such a scheme permits one to achieve very strong and homogeneous focusing of positrons, for a wide range of positron energy (Table 1). The second point is the possibility of using the traditional scheme for electron cooling (see Sections 5 and 6). Finally, the reducing of the magnetic field in the positron source area and its compression in the recombination area enables one to get a colder and denser positron beam and to enhance the recombination rate (Section 8).

The disadvantage of this scheme is that the positron beam does not change its size during the cooling procedure. There is a big temptation to place the positron source outside the solenoid [5], to have a positron beam compression during cooling. However, the transverse velocities of the positrons are so high here, that electron cooling does not work productively. Therefore the most effective way is to immerse a positron source (a target) in the magnetic field, to accept a positron beam emittance as high as possible and to use electron cooling for diminishing the angular spread in the positron beam to obtain a high recombination rate [6,7].

The analysis shows that the main practical limitation of the antihydrogen generation rate at LEAR is the lack of low energy positrons (see Section 4). The case of a very intense positron beam limited only by its space charge was discussed in Ref. [6].

For experiments with antihydrogen a low particle energy is preferable [8], therefore two cases are considered below – the \bar{p} energy, conventional for LEAR – 50 MeV, and the lowest energy, achievable at LEAR – 0.5 MeV. A possibility to reach very low energy, of the order of 100 keV, and \bar{H}^0 -trapping is also discussed (Section 9).

3. The recombination rate

The rate of \bar{H}^0 generation is described by the formula

$$R \equiv \frac{dN}{dt} = \frac{\alpha_r}{\gamma^2} \frac{N_p N^+}{C_p C^+} \frac{l_r}{\pi a^2}, \quad a = \max\{a_p, a^+\}, \quad (1)$$

where α_r is the recombination coefficient [2,9]:

$$\alpha_r = \frac{20\alpha r_e^2 c^2 L_c}{V}, \quad V = \sqrt{(V_p)^2 + (V^+)^2}, \quad (2)$$

N_p, N^+ are the antiproton and positron beams intensities, a_p, a^+ the radii of their cross-sections, C_p, C^+ the circumferences of the antiproton and positron rings, l_r the recombination region length, V_p, V^+ the antiproton and positron velocities in the particle rest frame, $\alpha = 1/137$, r_e the electron classical radius, $L_c = \ln(\alpha c/V)$, $\gamma = (1 - \beta^2)^{-1/2}$, $\beta = v_0/c$, v_0 the average particle velocity in the laboratory frame.

The standard LEAR storing, deceleration and cooling procedure yields a beam at an antiproton energy 50 MeV with an intensity of about 10^{10} particles and the emittance $\pi\epsilon \sim 3\pi \text{ mm} \cdot \text{mrad}$ [10]. One can hope, that the \bar{p} -beam intensity can be increased up to 1×10^{11} with a very cold \bar{p} -beam: $\epsilon_v \approx \epsilon_H \approx 0.5\pi \text{ mm} \cdot \text{mrad}$. It corresponds to $V_p \sim 3 \times 10^6 \text{ cm/s}$ and $a_p \sim 1.5 \text{ mm}$.

The optimal scheme parameters correspond, obviously, to equal transverse dimensions for the positron and antiproton beams

$$a = a_p = a^+, \quad (3)$$

when no “spare” particles are circulating in either ring. The positron velocities V^+ in the cooled positron beam are at least of the order of the electron transverse velocities in the cooling electron beam, if the intensity of the positron beam is low enough. Thus, $V^+ \sim \sqrt{2T_\perp/m} \sim 1.5 \times 10^7 \text{ cm/s}$ and does not depend strongly on particle energy (because the electron transverse temperature T_\perp is defined mainly by the cathode temperature). Therefore one can neglect V_p in Eq. (2).

One can obtain a certain increase of the recombination rate by using bunched beams of antiprotons and positrons. Especially, this gives a significant gain, when the particle number is rather small. In the case of bunched beams the parameter C_p in Eq. (1) should be replaced by the maximum bunch length

$$l_b = \max\{l_p, l^+\}.$$

We suppose $l_r > l_b$ and $C^+ < C_p$. Therefore, the gain in the recombination rate is by a factor of

$$g_1 = C_p/l_b \approx 50.$$

The bunched beam regime can be used until the intensity of the beams is lower than the space charge limit. If this limit is reached, one can use the multibunch regime in the antiproton ring with bunch number

$$n_b \leq C_p/C^+,$$

where n_b is an integer. The productivity in the multibunch regime is n_b times higher, than in the single bunch one:

$$g_n = n_b C_p/l_b.$$

One can meet, of course, some problems in bunched beam regimes because of the particle momentum spread increas-

Table 1
The recombination rate with cooled \bar{p} - and e^+ -beams

p-beam		
energy [MeV]	50	0.5
intensity	1×10^{11}	1×10^9
radius [mm]	1.5	1.5
e ⁺ -beam		
energy [keV]	27.2	0.27
intensity	1×10^9	1×10^8
\bar{H}^0 generation rate [atoms/s]	3×10^4	30

ing. However, one can hope, that with efficient cooling and modest beam intensities these problems can be avoided.

The estimation of the \bar{H}^0 generation rate for unbunched beams, $C^+ = 19.65$ m, $l_r = 1.5$ m are presented in Table 1.

4. The positron source

The problem of low energy positron production constitutes the main limitation of \bar{H}^0 generation rate. Three methods for the production of such positrons are known at present:

1) a linear accelerator with an electron beam bombarding a target at an electron energy of about 40 MeV; positrons, produced in the depth of the target, travel to its surface and slow down [8,11,12];

2) a source of hard synchrotron radiation with a photon energy above the pair generation threshold [13];

3) a strong radioactive source [14].

The second method very attractive (see Table 2) is, but it seems unrealizable at the CERN facility. The third method was the obvious disadvantage of high radioactive in use.

The energy spread of positrons, emitted by the target, is a few eV, and they can be accelerated up to the chosen energy ε_0 , by putting the target under the corresponding positive potential. After such electrostatic acceleration the positron longitudinal momentum spread, and the longitudinal temperature in the particle rest frame reduce significantly. However the transversal temperature is conserved and has the same value T_t as at the target (see Ref. [6]):

$$T_{\parallel} = \frac{T_s^2}{2\varepsilon_0}, \quad T_{\perp} = T_t \sim 1 \text{ eV}. \quad (4)$$

To decrease the last one, one can use electron cooling [5–7].

Table 2
The comparison of slow positron sources

Primary particle	e^-	γ	A*
Primary particle energy [MeV]	40	1.2	—
Conversion efficiency $N^+/N_{e,\gamma}$	1×10^{-7}	3×10^{-5}	1
Available e^+ flux, [s ⁻¹]	1×10^8	2×10^{12}	1×10^6

5. The electron cooling of positrons. A general description

The use of electron cooling of the positrons is the first decisive specificity of this proposal. It can be described with the same well known formulae [1,5], which are used for heavy particle electron cooling, by substituting the electron (positron!) mass instead of the proton (ion) one and to add in the dominator a factor 2, taking into account the “technical” (reduced) mass of electron–positron colliding particles (see Ref. [5]):

$$\tau_{ee} = \frac{\beta^4 \gamma^5}{8\pi c r_e} \frac{mc^3}{\eta_e e J_e} \frac{1}{L_c} (\theta^+)^3 N_{col}^{-1}. \quad (5)$$

Here r_e , m are the electron classical radius and mass, J_e the electron beam density (when the electron beam cross section exceeds the positron beam one), L_c the Coulomb logarithm, θ^+ the angular spread in the positron beam, η_e the ratio of the cooling section length to the positron ring circumference, N_{col} is the effective number of electron–positron collisions (see Eq. (6) below). This formula at $N_{col} = 1$ corresponds only to so called “fast collisions” (see Ref. [6]) and neglects the effects of electron and positron magnetization. So, it is the upper limit for the cooling time. For parameters chosen here (see Table 3) the Coulomb logarithm decreases as the positron velocity decreases in the range 17–8.

If electrons and positrons are immersed in a magnetic field, the collisions between them can repeat a few times during one interaction event [5] due to rotation around a magnetic field line. The number of such multiturn collisions is equal, by order of magnitude, to

$$N_{col} = \frac{\omega_B \tau_{int}}{2\pi}, \quad \tau_{int} = \min \left[\frac{1}{v_0}, \frac{\rho_L}{\langle |V^+ - V_{e\parallel}| \rangle} \right]. \quad (6)$$

Here τ_{int} is the characteristic interaction time, ω_B , ρ_L the particle Larmor frequency and Larmor radius in the magnetic field B , V^+ , V_e the particle velocities in the particle rest frame, l the cooling section length. This effect can decrease the cooling time significantly if the positron electrostatic acceleration is used [Eq. (4)]:

$$N_{col} \sim \sqrt{2\varepsilon_0/T_t} \sim 5-8. \quad (7)$$

A few effects limit the equilibrium temperature and the lifetime of the cooled positron beam. They are multi- and single-scattering of positron in the residual gas, energy exchange between positrons and antiprotons (the same electron cooling mechanism, that transfers energy from positrons to antiprotons or back during this internal in the recombination region), intrabeam scattering. The influence of all these effects is negligible in the presence of strong electron cooling.

Table 3

The general parameters of the positron storage ring

Electron and positron energy [keV]	27		0.27
Circumference [m]		19.65	
Toroid radius [m]		1.0	
Straight section length [m]		2×1.5 2×3	
Longitudinal magnetic field [G]	600		60
Larmor radius [cm]		0.85	
Electron beam			
diameter [mm]		3	
beam current density [A/cm^2]	1		0.002
Positron beam			
intensity	1×10^9		1×10^8
current [μA]	750		7.5
energy spread of the target [eV]		3	
beam diameter [mm]		3	
injection angular spread [mrad]	10		100
angular spread after cooling [mrad]	2		20
Vacuum pressure [Torr]	1×10^{-10}		1×10^{-10}
Characteristic times:			
at injection			
electron cooling [μs]	2		300
positron multiscattering [ms]	25		2.5
at equilibrium state			
positron multiscattering [ms]	320		32

5.1. The generation of positronium

The positron lifetime is also limited by recombination with electrons in the cooling region of the positron ring, and the positron beam intensity decreases due to this recombination with a characteristic time, which is analogous to $\bar{p}e^+$ recombination:

$$\tau_{\text{pos}} = N^+ / R_{\text{pos}}, \quad (8)$$

where R_{pos} is given by Eqs. (1) and (2), with the exchange $V_p \rightarrow V^+$ and multiplication of α_r by 4 (the technical mass squared). One should note, that the e^+e^- recombination orthopositronium production prevails, and its lifetime is 0.14 μs , or the flight length – 14 m, when particle velocity is about 10^{10} cm/s. The parapositronium lifetime is 0.125 ns, and the flight length – 1.2 m. This means that the cooling section of the positron ring is a source of orthopositronium, which gives additional possibilities for physics experiments.

5.2. Equilibrium state

When the heating effects, mentioned above, are negligible, the equilibrium temperature of the positrons at low intensity is defined by the cooling process.

The cooling of magnetized positrons by magnetized electrons, which takes place in the case under discussion, has some disadvantages compared to heavy particles. The

latter can be cooled down to the longitudinal electron temperature [6], because they do not feel the magnetic field influence. By contrast, magnetized positrons have in the equilibrium state a nonuniform velocity distribution [5]:

$$T_{\perp}^+ \rightarrow (T_e)_{\perp}, \quad T_{\parallel}^+ \rightarrow (T_e)_{\parallel}. \quad (9)$$

Thus, one can admit

$$V^+ \sim \sqrt{2(T_e)_{\perp} / m} \sim 3 \times 10^7 \text{ cm/s}. \quad (10)$$

6. The positron ring

In the proposed scheme the positron ring (Fig. 2) has four toroidal solenoids and four straight ones. The latter are used for the injection/extraction of electrons and positrons, the electron cooling of positrons and the production of $\bar{p}e^+$ recombination.

For estimations we choose a magnetic field strength equal to the field in the LEAR e-cooler, which is about 600 G.

6.1. The electron/positron beams superposition and separation. Positron injection

This problem is complicated enough in the presence of a longitudinal magnetic field. The most effective way is, in our opinion, to use the centrifugal drift of particles in

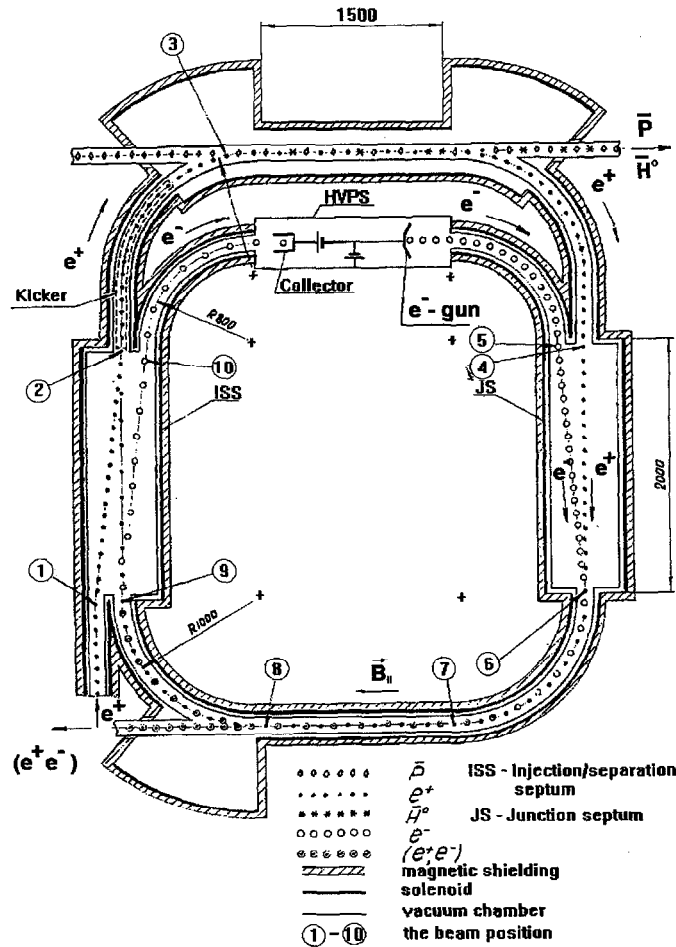


Fig. 2. The layout of the positron ring. ISS – injection/separation septum; JS – junction septum; HVPS–high voltage power supply. All the dimensions are given in mm.

toroids. The particle drift velocity is directed along the toroid axis and is equal to [15]

$$v_{cf} = \frac{\beta^2 \gamma m c^3}{e B R} = \frac{\rho_L}{R} \beta c, \quad (11)$$

where R is the toroid radius (Fig. 3), ρ_L the Larmor radius of the particle. It follows from Eq. (11) that the particle displacement, caused by drift, depends only on the bending angle θ_0 in the toroid and the particle Larmor radius:

$$\Delta_{cf} = \theta_0 \rho_L \quad (12)$$

and does not depend on the bending radius ($BR = \text{const.}$ in a toroidal coil!). This peculiarity of such a method of a particle displacement is very important and makes it differ in principle from other methods. Particularly, the magnitude of the particle displacement in crossed transverse electrostatic and longitudinal magnetic fields depends on

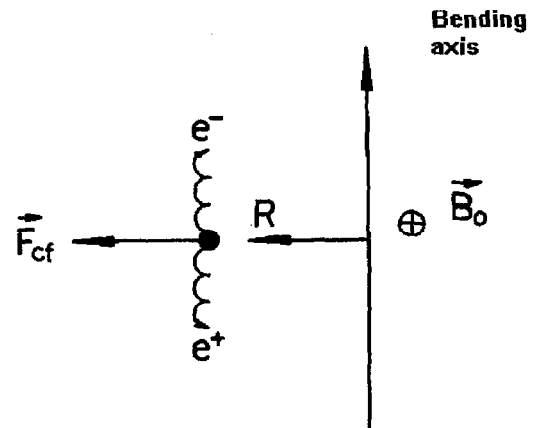


Fig. 3. The scheme of centrifugal drift.

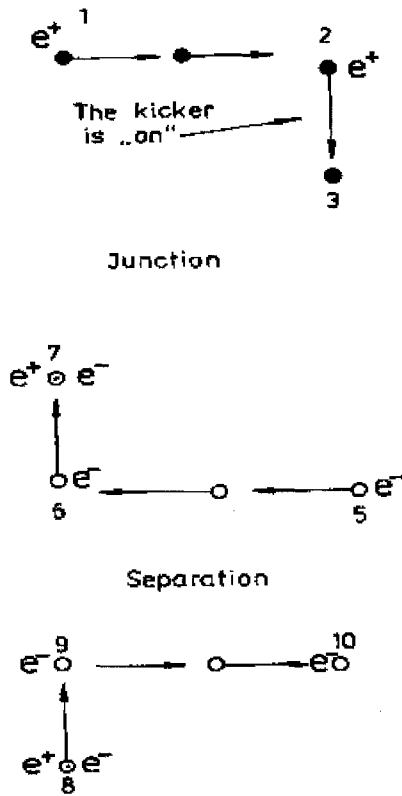


Fig. 4. The scheme of particle motion in cross-section plane of the septums.

the particle transverse coordinate, because particle energy changes after entering an electric field.

The centrifugal drift can perturb particle motion and induce some transverse velocity. If entrance into a toroidal magnetic field is adiabatic (when the length of the transition region from the straight solenoid field to the toroidal one is much larger of Larmor radius ρ_L), such a perturbation is negligible:

$$\Delta V^+ \leq v_0 \frac{a_0 r}{\rho_L^2} e^{-r/\rho_L}. \quad (13)$$

Here r is the radius of the solenoid coil, a_0 the positron beam radius.

If the positron drift is compensated for by application of

a transverse bending field, the electron displacement is twice as large: $\Delta_{\text{tot}} = 2\Delta_{\text{cr}}$.

The same principle is used for positron beam injection. Positrons are generated by some positron source and travel along a solenoid magnetic field to the entrance into the positron ring (Fig. 2, position 1). Here the positron beam is located to the left of the central trajectory in the ring and above its median plane (Figs. 4 and 5, position 1). Then it comes into the septum, which is a superposition of longitudinal B and transverse (horizontal) B_H magnetic fields (Fig. 5). Here positrons have a horizontal displacement to the right

$$\Delta_{\text{septum}} = (B_H/B)L_{\text{septum}} \quad (14)$$

and come to position 2 at the toroid entrance (see Figs. 2, 4 and 5). Then they travel in a toroidal magnetic field and an additional vertical magnetic field of a *kicker*.

Let us suppose that the kicker field is directed downwards and it is just equal (in absolute value) to the bending field for positron trajectory radius R (this field must be directed up). Then positrons move down in agreement with Eq. (12) and come to position 3 in the median plane. From this point, the positrons travel along the central trajectory of the ring and do not feel any influence of the septum field due to the *septum design* (Fig. 5).

When single-turn injection of positrons is over, the *kicker field* changes its direction. This procedure seems not too complicated because of the long revolution period of positron in the ring (200 ns for 27 keV positrons). If the switch time of the kicker is equal to 20 ns, the *induction voltage* on the kicker is about 5 kV.

Now we discuss the electron beam motion. Electrons travel from the gun (Fig. 2) to the junction section (Figs. 2, 4 and 5, position 5). Here the electron beam is below the median plane and to the right of the central trajectory. In the horizontal field of the *junction septum* and the longitudinal field of the solenoid the beam displaces to position 6. If the bending field in the toroid directs the positrons along a toroid magnetic line, it will cause the drift of electrons. Drifting up, they come to the central trajectory at position 7 – junction is over! *Electron cooling* of the positron occurs between positions 7 and 8. Thereupon electrons displace up again to position 9 in the next toroid, to the right in the *injection/separation septum* and come to the collector.

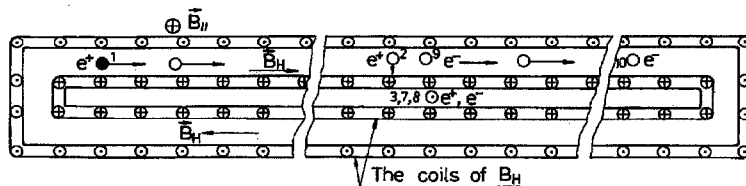


Fig. 5. The cross-section of the septum.

6.2. The positron motion stability

The proposed focusing system is very similar to the “stellarator” one, well known in plasma physics (see, for instance, Ref. [16]). The difference is the significant magnitude of the longitudinal components of the positron momentum. In principle, one can create a very precise equilibrium trajectory for a single particle – let us say, on the axis of the positron beam. However, some disagreement between the momentum of the unaxial particle and the bending (dipole) magnetic field in toroids always exists. The toroidal magnetic field also has some radial gradient. Both these reasons significantly decrease the centrifugal drift, in comparison with the full value [Eq. (11)], when the bending field is on. Nevertheless, this slow drift can limit the particle lifetime in the ring. The method to avoid this problem is known from stellarator experience: one has to superimpose few couples of spiral conductors with opposite current directions on the torus solenoid (Fig. 6).

In such a solenoid a magnetic field line has the form of a spiral, wrapped around a toroidal surface, coaxial with the torus, if the conductor currents generate a quadrupole magnetic field with sufficiently large gradient G . The particle motion is stable in such a field even with some disagreement ΔB_{\perp} between the particle momentum p and the bending magnetic field B_{\perp} , if the gradient magnitude satisfies the condition [7]:

$$\text{Max} \left\{ \sqrt{\frac{q\rho_L}{R}}, \sqrt{\frac{qR}{a_0}} \Delta \right\} \ll \frac{GR}{B_0} \ll 2q, \quad (15)$$

where $2\pi/q$ is the angular period of the spiral winding, R the radius of the torus, a_0 the positron beam radius, $\Delta = \Delta B_{\perp}/B_{\perp}$. The positrons have an additional angular spread because of motion in such a field, equal to

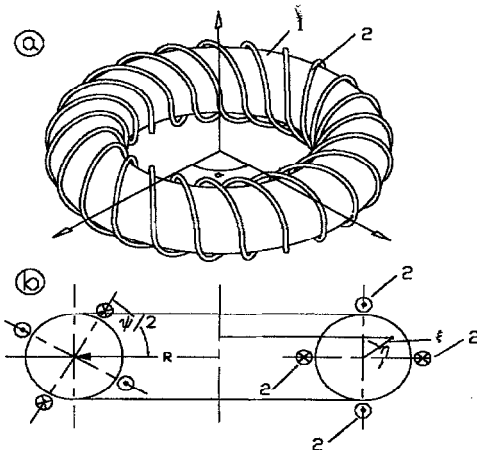


Fig. 6. The magnetic system (a) and its cross-section (b). 1 – torus coil; 2 – spiral winding.

$$(\Delta\theta^+)^2 \approx 8 \left(q\Delta \frac{pc}{eGR^2} \right)^2 + \left(\frac{2a_0\rho_L}{R^2} \right)^2. \quad (16)$$

One can expect, in principle, the appearance of resonance phenomena, similar to the ones that take place in the particle motion in conventional storage rings. However, this problem needs closer examination, which is in progress now. The analysis of particle motion in the stellarator field [16] shows that the spiral winding with two couples of conductors is preferable from this point of view. The experience of operation of stellarator machines allows us to hope that the achievement of stable positron motion is possible. One should note also that positron and electron beam space charge may be a contributory factor to the stability.

A special question is that of positron motion stability in a storage ring of racetrack form, having straight sections. One prefers to avoid spiral winding in these sections. Then the magnetic field configuration receives a perturbation, the length of which seems to be of the straight section size l . However, the real perturbation takes place in the transit region only – between the toroidal and the straight parts of the solenoid and its length is of the order of the solenoid coil radius r . If the condition of adiabaticity, $\rho_L \ll r$, is represented, the influence of this transit area is small [see Eq. (13)].

6.3. Multiple single-turn injection and storing of positrons

The low intensity of the positron source sets one using positron storing. And the only possibility that remains in the case of longitudinal magnetic field is to use storing in longitudinal phase space. The single-turn injection, described in Section 6.1, can be used then, together with continuous electron cooling [19]. Such a method needs some radio-frequency accelerating system, but of very modest parameters. Actually, the RF voltage for separatrix, accepting a full energy spread of the positrons at injection, is

$$V = \pi T_{\parallel}^+ / e \sim 10 \text{ V}. \quad (17)$$

The analysis shows [7] that the phase stability of the particle motion in such a magnetic system and RF-accelerating field takes place definitively, if the magnetisation condition (15) is respected. In this case the transition energy factor is equal to

$$\gamma_{tr} = \frac{R}{2q\rho_L} \left(\frac{GR}{B_0} \right)^2 \gg 1. \quad (18)$$

The e^+ storing rate is limited mainly by the source parameters and cooling time value. One example, based on results from Refs. [9,10], is presented in Table 4.

Table 4
The positron storing rate

Positron energy [keV]	27	0.27
e^+ revolution period [μ s]	0.21	2.1
Injection repetition rate [s]	10^4	10^3
e^+ number per injection cycle	10^4	10^4
Storing time for 10^8 [s]	1.0	10.0

7. Vacuum condition

One can see from Table 3, that the requirements imposed on the vacuum pressure are not very strict: even at $P = 1 \times 10^{-10}$ Torr the characteristic time for multiscattering is much larger than the electron cooling time at injection. And the situation is even much better for a cooled e^+ -beam.

8. The transporting of e^+ -beam. Magnetic field variation

So long as the source is immersed in a longitudinal magnetic field the transportation of positrons from the source to the ring can be performed also in a long solenoid with a low magnetic field, of about 60–200 G. The transportation solenoid can be bent in any necessary direction and it can have some gaps in the winding for vacuum pumps, probes etc.

The adiabatic expansion or compression of the solenoid magnetic field in the ring can bring some gain in the recombination rate. So, if the magnetic field magnitudes are, respectively, B_t on the positron source, B_{gun} in the electron gun, B_{cool} , B_{rec} in the cooling and recombination sections, the positron equilibrium temperature and positron beam size in the recombination section are equal to

$$T_{rec}^+ = \frac{B_{rec}}{B_{cool}} (T_e)_\perp \sim \frac{B_{rec}}{B_{gun}} T_{cathode},$$

$$(a_{rec}^+)^2 = \frac{B_t}{B_{rec}} (a_t^+)^2. \quad (19)$$

This gives the gain, comparatively to Eq. (1), is approximately equal to

$$K_{gain} \sim \frac{\sqrt{B_{rec} B_{gun}}}{B_t}. \quad (20)$$

This means that some gain can be obtained by increasing B_{rec} , B_{gun} and decreasing B_t .

9. Some possibilities for slow \bar{H}^0 -atoms generation

For certain applications very slow \bar{H}^0 -atoms are desirable (see, for instance, the review [8]). They can be

generated with the proposed scheme, by using, for instance, very strong deceleration of the antiprotons before they enter the recombination section. For this purpose the positron ring as a whole, including the positron source target, is to be placed under a high negative potential U_d , whose magnitude depends on the \bar{H}^0 -atom energy $\varepsilon_{\bar{H}}$. To decelerate positrons up to the kinetic energy

$$\varepsilon_s = (m/M) \varepsilon_{\bar{H}}, \quad (21)$$

one can place inside the recombination section a metallic tube that has the potential U_0 . For chosen $\varepsilon_{\bar{H}}$ and satisfying Eq. (21), we find:

$$U_d = -\frac{1}{e} \left(\varepsilon_p + \varepsilon_0 - \left(1 + \frac{m}{M} \right) \varepsilon_{\bar{H}} \right), \quad (22)$$

$$eU_0 = \varepsilon_0 - \frac{m}{M} \varepsilon_{\bar{H}}. \quad (23)$$

Here ε_p , ε_0 are the kinetic energy of the circulating antiprotons and positrons, respectively.

The main limitation of the $\varepsilon_{\bar{H}}$ value is the stability of the circulating beams, which have very low velocity in the recombination section. One can roughly estimate the influence of the effect on the antiproton ring tune shift:

$$\Delta Q \sim \frac{r_p N_p l_r}{4\pi Q \beta^2 a^2}, \quad (24)$$

where r_p is the proton classical radius, Q the betatron number. For $\varepsilon_p = 50$ keV ($\beta \approx 0.01$), $N_p = 3 \times 10^8$, $Q = 3$, $l_r = 1.5$ m, $a = 1.5$ mm it gives $\Delta Q = 0.1$. Such a tune shift is admissible for the particle beam, when electron cooling is used. The \bar{H}^0 -atom generation rate in this case will be about a few atoms/s, if the positron intensity is kept at the level of 1×10^8 (see Table 1).

One can expect even an achievement of lower energy, however speculations here are very uncertain, and further consideration and an experimental study is necessary.

The influence of the longitudinal magnetic field of the positron ring on antiproton dynamics becomes quite large at low antiproton energy and requires also more accurate study.

The limitations of the positron beam intensity in the scheme does not look so severe, as for the antiproton one: the focusing system with a longitudinal magnetic field permits the slowing down of particles up to a few eV, and experience with plasma machines, such as the stellarator and tokamak, prove this fact.

When such a low energy of antihydrogen atoms is achieved, one can hope to succeed in injecting them into a trap [1] and cooling down, by laser cooling, to a temperature that permits the performing of the ultimately precise experiments, as done with hydrogen atoms (see details in Ref. [8]).

10. Conclusion

The level of the generation rate that can be achieved with the proposed scheme, has practical interest: $R \approx 3 \times 10^4$ –30 atom/s for a wide range of energy. Some improvements can be made, like expanding the magnetic field in the cooling section and its compression in recombination area. These can increase the \bar{H}^0 yield by a few times.

Acknowledgements

We wish to thank B. Chirikov and V. Volosov, who drew our attention to the possibility of the positron motion stabilisation and gave much advice, to J. Bosser, M. Charlton, Ya. Derbenev, G. Kulipanov, D. Moehl and L. Rinolfi for fruitful discussions, and to J. Eades and L. Montanet for their interest in this work.

References

- [1] G.I. Budker and A.N. Skrinsky, *Sov. Phys.-Usp.* 21 (1978) 277;
N.S. Dikansky, I.N. Meshkov and A.N. Skrinsky, *Nature* 276 (1978) pp. 736.
- [2] H. Poth, *Appl. Phys. A* 43 (1987); CERN-EP/90-04 (1990).
- [3] G. Baur, G. Boero, W. Oelert et al., *Phys. Lett. B* 368 (1996) 251.
- [4] H. Herr, D. Moehl and A. Winnacker, in: *Physics at LEAR with Low Energy Cooled Antiprotons* (Plenum Press, New York, 1982) p. 659.
- [5] A.S. Artamonov, Ya.S. Derbenev and E.L. Saldin, *Part. Accel.* 23 (1988) 79.
- [6] I.N. Meshkov and A.N. Skrinsky, Report on 3rd Biennial Conf. on Low-Energy Antiproton Physics, September 1994, Bled, Slovenia;
I.N. Meshkov, *Particles and Nuclei* 25 (6) (1994).
- [7] I.N. Meshkov and A.N. Skrinsky, Preprint JINR E9-95-130, Dubna, (1995).
- [8] M. Charlton, J. Eades, D. Horvath, R.J. Hughes and C. Zimmermann, *Phys. Rep.* 241 (2) (1994) 65.
- [9] M. Steck et al., *Proc. 3rd European Part. Conf.*, Vol. 1 (1992) pp. 827–829.
- [10] J. Bosser, M. Chanel, R. Ley and G. Tranquille, Ref. [7], pp. 845–847.
- [11] F. Ebel, W. Faust, C. Hahn et al., *Nucl. Instr. and Meth. A* 272 (1988) 626.
- [12] J. Paridaens, D. Segers, M. Dorikens and L. Dorikens-Vanpraft, *Nucl. Instr. and Meth. A* 287 (1990) 359.
- [13] G.N. Kulipanov, N.A. Mezentzev and A.N. Skrinsky, *Rev. Sci. Instr.* 63 (1992) 289.
- [14] M. Charlton and G. Laricchia, *Hyp. Interact.* 76 (1993) 97.
- [15] V. Kudelainen, I. Meshkov and R. Salimov, Preprint INP 72–70, Novosibirsk, (1970), translated in CERN-PS/77-08 (1977).
- [16] A.I. Morozov and L.S. Soloviev, in: *The problems of the Plasma Theory* (in Russian), Vol. 2 Atomizdat, Moscow, (1963) pp. 3–91.
- [17] B.V. Chirikov, *Sov. Dokl. Akad. Nauk* 174 (1967) 1313.
- [18] G.I. Budker, in: *The Plasma Physics and the Problem of Controlled Thermonuclear Reactions* (in Russian) vol. 1 (USSR Academy of Sciences, Moscow, 1998) pp. 66–74.
- [19] Heavy Ion Storage Ring Complex K4-K10, A Technical Proposal, ed. G.M. Ter-Akopian, JINR, Dubna (1992) pp. 23–25.